Langmuir

ARTICLE

pubs.acs.org/Langmuir

Surface Rheology of Saponin Adsorption Layers

R. Stanimirova,[†] K. Marinova,[†] S. Tcholakova,[†] N. D. Denkov,*[,†] S. Stoyanov,[‡] and E. Pelan[‡]

[†]Department of Chemical Engineering, Faculty of Chemistry, Sofia University, 1 J. Bourchier Avenue, 1164 Sofia, Bulgaria

[‡]Unilever R&D, Vlaardingen, The Netherlands

Supporting Information

ABSTRACT: Extracts of the *Quillaja saponaria* tree contain natural surfactant molecules called saponins that very efficiently stabilize foams and emulsions. Therefore, such extracts are widely used in several technologies. In addition, saponins have demonstrated nontrivial bioactivity and are currently used as essential ingredients in vaccines, food supplements, and other health products. Previous preliminary studies showed that saponins have some peculiar surface properties, such as a very high surface modulus, that may have an important impact on the mechanisms of foam and emulsion stabilization. Here we present a detailed characterization of the main surface properties of highly purified aqueous extracts of *Quillaja* saponins. Surface tension isotherms showed that the purified *Quillaja* saponins behave as nonionic surfactants with a relatively high cmc (0.025 wt %). The saponin adsorption isotherm is described well by the Volmer equation, with an area per molecule of close to 1 nm^2. By comparing this area to the molecular dimensions, we deduce that the hydrophobic triterpenoid rings of the saponin molecules lie parallel to the air−water interface, with the hydrophilic glucoside tails protruding into the aqueous phase. Upon small deformation, the saponin adsorption layers exhibit a very high surface dilatational elasticity (280 ± 30 mN/m), a much lower shear elasticity (26 ± 15 mN/m), and a negligible true dilatational surface viscosity. The measured dilatational elasticity is in very good agreement with the theoretical predictions of the Volmer adsorption model (260 mN/m). The measured characteristic adsorption time of the saponin molecules is 4 to 5 orders of magnitude longer than that predicted theoretically for diffusion-controlled adsorption, which means that the saponin adsorption is barrier-controlled around and above the cmc. The perturbed saponin layers relax toward equilibrium in a complex manner, with several relaxation times, the longest of them being around 3 min. Molecular interpretations of the observed trends are proposed when possible. Surprisingly, in the course of our study we found experimentally that the drop shape analysis method (DSA method) shows a systematically lower surface elasticity, in comparison with the other two methods used: Langmuir trough and capillary pressure tensiometry with spherical drops. The possible reasons for the observed discrepancy are discussed, and the final conclusion is that the DSA method has specific problems and may give incorrect results when applied to study the dynamic properties of systems with high surface elasticity, such as adsorption layers of saponins, lipids, fatty acids, solid particles, and some proteins. The last conclusion is particularly important because the DSA method recently became the preferred method for the characterization of fluid interfaces because of its convenience.

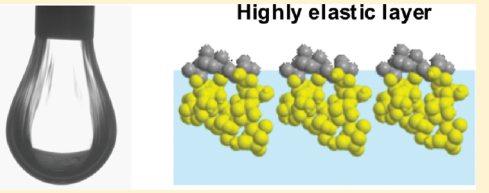

1. INTRODUCTION

Saponins are natural surface-active substances (surfactants) present in more than 500 plant species.[1,2] Saponin molecules contain a hydrophobic part, composed of a triterpenoid or steroid backbone, and a hydrophilic part consisting of several saccharide residues, attached to the hydrophobic scaffold via glycoside bonds (Figure 1).Terpenoid saponins are usually found in dicotyledonous plants, and the steroid saponins are usually found in monocotyledonous plants.[1,2]

The diversity of amphiphilic structures of the saponin molecules determines their rich physicochemical properties and biological activity. The surface activity of the saponins serves as a basis for their traditional use in food production[3−6] and in other industrial applications.[7−9] In recent years, various new applications have emerged in medicine,[10−17] the food industry,[2,6,16,17] cosmetics,[8,18−20] and energy production.[21] Saponins are currently used as foamers and emulsifiers in beer and soft drinks,[2,5] as solubilizing agents for vitamins[16] and minerals[17] in food additives, and as key ingredients in technology for decreasing the cholesterol level in foods (oils, milk, butter, and others).[2,3] The saponins serve as stabilizers of cosmetic emulsions, as foam boosters in shampoos and conditioners, and as skin antiaging actives.[8,18−20] The saponins are used as adjuvants in vaccines,[9,13] they exhibit noticeable antitumor activity,[14,15] and they have some antiallergic and antiseptic action.[2] The saponins in food were reported to decrease cholesterol levels in the bloodstream,[10,11] with a noticeable decrease in the risk of cardiovascular diseases.[12] In summary, the saponins uniquely combine the properties of surfactants and essential bioactive ingredients, which makes them particularly attractive for various technologies.

These applications and the nontrivial physicochemical properties of saponins have recently sparked increasing research activity.

Received: July 24, 2011
Revised: September 6, 2011
Published: September 06, 2011

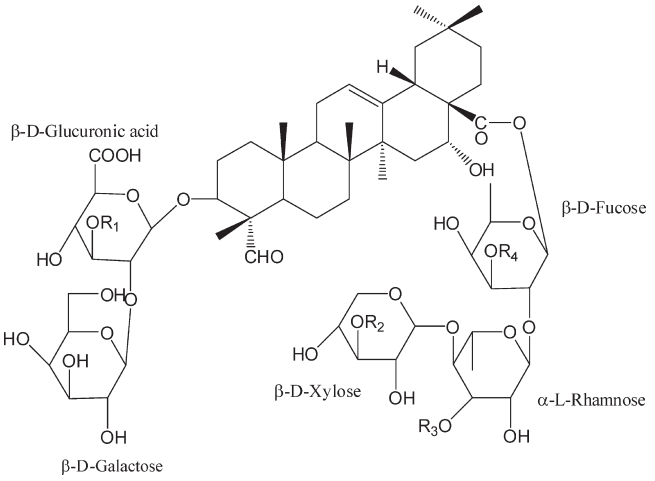

Figure 1. General molecular structure of *Quillaja* saponins. Notation R1−R4 represents either H or different sugar groups.

Because of their amphiphilic nature, saponin molecules form aggregates (micelles) in aqueous solutions. The size, shape, and structure of the saponin micelles depend on their plant origin, temperature, pH, electrolyte concentration, and so forth.[2,22−26] Experiments showed that micellar solutions of saponins, extracted from the South American tree *Quillaja saponaria*, are efficiently able to solubilize very large hydrophobic molecules such as cholesterol, phytosterols, phenanthrene, and others, and this property of the *Quiallaja* saponins is essential for their application in some of the technologies mentioned above.[24,25]

As known, many important foam and emulsion properties, such as stability during formation and shelf storage,[27−29] and rheological properties[30] are governed by the properties of the adsorption layers (formed on bubble or drop surfaces) that stabilize the respective foam and emulsion films. Despite the wide technological applications of saponins, the properties of the saponin adsorption layers and the related mechanisms of foam and emulsion stabilization are still poorly understood.[2,26] Systematic data for the foamability of saponin solutions are scarce, and the results are presented at a purely phenomenological level[31] without attempting to clarify the mechanisms of foam stabilization and the role of surface properties. The emulsifying capability of saponins has not yet been investigated systematically. In recent years, only a few papers have been published that empirically describe the applications of saponins for the stabilization of macroemulsions[32] and coal-oil mixtures without a mechanistic study of the phenomena involved.[21] This situation is largely due to the specific difficulties when working with natural extracts; they often contain a complex mixture of different ingredients (proteins, polysaccharides, etc.) with nontrivial interactions between them.

Several studies were published recently that consider saponin adsorption layers[33,34] and saponin-stabilized foam films.[35] In a recent paper, Anton and Bouriat[35] showed experimentally that the properties of saponin-stabilized foam films are rather different from those of films stabilized by synthetic surfactants or proteins. For example, in the process of foam film formation with saponins, a liquid lens (dimple) is trapped in the film center, with subsequent slow drainage of the liquid from the film and simultaneous dimple fragmentation into numerous small lenses. These lenses have large contact angles at their periphery, which indicates a very strong attraction between film surfaces.[35] The specific dynamics of the saponin-stabilized films indicates peculiar rheological properties of the saponin adsorption layers, with an expected strong impact on the overall foam and emulsion properties (stability, rheology, drainage, etc.).[30] Indeed, preliminary measurements aimed at comparing the surface rheological properties of the adsorption layers from several natural surfactants showed rather high surface dilatational elasticity with saponins.[33] In another recent study,[34] the kinetics of adsorption of saponin molecules was studied and the conclusion was reached that adsorption is a complex process with mixed diffusion-barrier control. Concluding this review, no systematic study of the surface rheological properties of the saponin solutions and of their relation to the foam and emulsion characteristics has been presented so far.

Therefore, the major aim of this study is to characterize the adsorption layers of highly purified *Quillaja* saponins with respect to (1) surface tension isotherms, (2) surface rheological properties, and (3) the kinetics of saponin adsorption and desorption. Saponin extracts from *Quillaja saponaria* are studied because these extracts are industrially produced, are available in high purity, and are widely used in various applications.

The article is organized as follows. Section 2 describes the materials and methods used. Section 3 presents the experimental results and a discussion. Section 4 summarizes the conclusions.

2. MATERIALS AND METHODS

2.1. Materials. We investigated three samples of *Quillaja* saponin extracts, all of them products of Desert King, Chile, obtained after different purification procedures. QL 1000 is the least purified sample and is a dark-brown liquid containing 9 wt % saponins. The color of the sample comes from natural phenols and tannins, which are extracted together with the saponins and other ingredients (polysaccharides and proteins) from the *Quillaja* tree; the saponins themselves are colorless. The second sample, a yellowish liquid extract containing 13 wt % saponin (commercial name QL Ultra), is purified by ultrafiltration to remove the polysaccharides, large proteins, and part of the polyphenols. The third sample, with the commercial name Supersap, is a white powder produced for pharmaceutical applications with a very high purity that contains 91 wt % saponins (the rest is ∼8 wt % moisture with traces of electrolytes and other organic ingredients). Most of the experiments were performed with Supersap solutions because this is the most pure sample of *Quillaja* saponins available on the market. To clarify the effect of the ingredients in the less purified samples, some comparative experiments were performed with QL Ultra and QL 1000.

All concentrations in the article are presented with respect to the actual saponin present in the solution. All solutions contain 0.01 wt % of the antibacterial agent NaN_3. For most of the solutions, the background electrolyte was 10 mM NaCl. To check for the effect of ionic strength, comparative measurements in the presence of 150 mM NaCl were performed with some samples. To check for the effect of Ca^{2+}, some measurements were made with solutions containing 1.2 mM $CaCl_2$ and 10 mM NaCl. The used salts were p.a. grade NaCl (Fluka), $CaCl_2$ hexahydrate (Fluka), and NaN_3 (Riedel-de Haën). For the calculations, we used 1650 g/mol for the average molecular weight of the saponins.[23]

All solutions were prepared with deionized water from a Milli-Q Organex purification system (Millipore, USA). The pH of the solutions was between 5.5 and 6.5 (without adjustment), except for the most concentrated (≥0.1 g/L) solutions of QL 1000 and QL Ultra, where the pH was ∼4. The lower pH of some saponin samples was ascribed to the presence of phosphoric acid in the batch.[32]

2.2. Methods for the Measurement of Surface Tension. The Wilhelmy plate method[36,37] was used to determine the equilibrium

surface tension, σ_e, of the solutions. The measurements were performed on a K100 tensiometer (Krüss GmbH, Hamburg, Germany) by using a platinum plate. Before each measurement, the plate was cleaned by heating in a flame, followed by abundant rinsing with deionized water.

Axisymmetric drop shape analysis (DSA) of pendant bubbles and drops was used to determine the dynamic surface tension, $\sigma(t)$, on the intermediate timescale (between 1 and 300 s) and the equilibrium tension, σ_e.[37−39] The measurements were performed on an Easy Drop automated instrument (Krüss GmbH, Germany).

The maximum bubble pressure method (MBPM) was used to compare the dynamic surface tension, σ(t), on a short timescale.[36−38] Measurements were performed on a BP2 automated bubble pressure tensiometer (Krüss GmbH, Germany).

The experimental methods that were used have a typical measuring accuracy of better than 0.1 mN/m. The reproducibility of the results in different experimental runs was better than ±0.5 mN/m. All measurements were performed at 25.0 ± 0.5 °C.

2.3. Experimental Techniques for the Characterization of Surface Rheological Properties of Adsorption Layers. A set of complementary experimental techniques were applied to characterize the surface rheological and adsorption/desorption properties of the adsorption layers.

Experiments with pendant drops were performed using the ODM/EDM module on a DSA 100 automated instrument (Krüss GmbH, Germany). Two measurement techniques were used: drop shape analysis (DSA) for pendant drops deformed by gravity[38−41] and capillary pressure tensiometry (CPT) with spherical drops.[42−45] The CPT method allows one to calculate the surface tension, σ, after measuring the capillary pressure difference, P_c, across the surface of a spherical drop with a radius of curvature of R.[42−45] Details of the method realization and the DSA and CPT procedures that were used can be found in refs 44 and 45.

The rheological properties of the adsorption layers were also studied with a model 302LL/D1 Langmuir trough (Nima Technology Ltd., U.K.). The area of the trough was varied with two parallel barriers that moved symmetrically at a predefined linear speed. The surface pressure was measured with a Wilhelmy plate made of chromatographic paper. The plate was positioned in the middle between the barriers and oriented either perpendicularly or parallel to the barriers.[46,47] All measurements were performed at 25.0 ± 0.5 °C.

Note that these different methods were needed because two of the well-established procedures (DSA and Langmuir trough) gave rather different results, as explained in section 3.2. Thus, we needed an independent method (CPT) to verify the conclusions drawn from our analysis of the possible reasons for the observed discrepancy.

2.4. Procedures for the Determination of the Surface Rheological Properties. Several types of surface deformations were applied, and the respective experimental results were analyzed by different models to obtain complementary information: sinusoidal oscillations of the area of pendant and spherical drops, triangle oscillations (with a constant rate of deformation) of the planar solution surface in the Langmuir trough, and deformation−relaxation measurements for both the drops and the planar surfaces. The parameters extracted from the different experiments and the methodology are described briefly below.

2.4.1. Surface Storage and Loss Moduli. These were determined from harmonic surface oscillations of deformed and spherical drops. In these methods, a sinusoidal variation of the drop surface area, A, is applied, with a defined angular frequency, ω (the respective oscillation period is $T = \omega/2\pi$), and amplitude, ΔA

$$A(t) = A_m + \Delta A \sin(\omega t) \tag{1}$$

where A_m is the mean drop area and t is time. Simultaneously, one measures the resulting variations of the surface tension, σ. For small area deformations, $\alpha = \Delta A/A_m$, and linear rheological behavior, the surface tension also oscillates sinusoidally:

$$\sigma(t) = \sigma_m + \Delta\sigma \sin(\omega t + \varphi) \tag{2}$$

Here σ_m is the mean value and $\Delta\sigma$ is the amplitude of σ variations, and φ is the phase shift of the oscillations of σ with respect to those of the area, A. The relation between $\sigma(t)$ and $A(t)$ can be presented as[38,43−45]

$$\Delta\sigma e^{i(\omega t + \varphi)} = E^*(\omega)\frac{\Delta A}{A_m} e^{i\omega t} \tag{3}$$

where E^* is the complex surface modulus $E^* = E' + iE''$ (here i is the imaginary number) and E' and E'' are the surface storage (elastic) and loss (viscous) moduli, respectively. The values of E' and E'' were obtained using the linear regression procedure described in ref 44.

2.4.2. Surface Dilatational and Shear Elasticities. These were determined from triangular surface oscillations applied in a Langmuir trough. Depending on the type of surface tension response, one can apply different procedures to analyze the experimental data and to extract information about the surface rheological properties.[46,47] For the elastic saponin layers studied here, we found it appropriate to use the approach developed in ref 46 in which two types of measurements are made, as described below, to determine both the dilatational and shear elasticities of the layers.

The area deformation in the Langmuir trough with two parallel barriers is unidirectional.[46,47] For such a deformation of solidlike adsorption layers, one should register different surface moduli when using a Wilhelmy plate oriented parallel or perpendicular to the direction of deformation.[46] The elastic stresses along the two main axes on the interface can be represented as[46]

$$\tau_j = K(\alpha_1 + \alpha_2) + 2\mu\left[\alpha_j - \frac{1}{2}(\alpha_1 + \alpha_2)\right], \quad j = 1, 2 \tag{4}$$

where α_1 and α_2 are the diagonal components of the strain tensor, τ_1 and τ_2 are the diagonal components of the stress tensor, index 1 refers to the direction parallel to the barriers, and index 2 corresponds to the direction perpendicular to the barriers. K and μ in eq 4 are the dilatational and shear elastic moduli, respectively. Note that eq 4 is written for negligible surface viscosity, which turned out to be a reasonable approximation for the saponin layers studied here when small surface deformations are applied. (See section 3.2 for an explanation.) In the case of unidirectional deformation, the deformation components are $\alpha_1 = \alpha = \ln(A/A_m)$ and $\alpha_2 = 0$. The reference area, A_m, coincides with the middle value of A during the oscillations. Thus eq 4 reads

$$\begin{aligned} \tau_1 &= \tau_{\parallel} = (K + \mu)\alpha \\ \tau_2 &= \tau_{\perp} = (K - \mu)\alpha \end{aligned} \tag{5}$$

When $\tau_{\parallel}$ and $\tau_{\perp}$ are measured at the same deformation α, eqs 5 can be rearranged to allow the direct calculation of the dilational, K, and shear, μ, moduli of elasticity from the stresses determined experimentally:

$$\begin{aligned} K &= \frac{1}{2}\left(\frac{\tau_{\parallel} + \tau_{\perp}}{\alpha}\right) \\ \mu &= \frac{1}{2}\left(\frac{\tau_{\parallel} - \tau_{\perp}}{\alpha}\right) \end{aligned} \tag{6}$$

2.4.3. Surface Dilatational Elasticity. This was also determined from the slope during the deformation period in the deformation−relaxation experiments, which were performed with spherical drops (in the expanding drop method) and planar surfaces (in the Langmuir trough).

In these types of experiments, a relatively large stepwise deformation is applied (deformation stage), after which the relaxation of the surface

tension toward its equilibrium value is measured (relaxation stage). During the period of surface deformation, one can measure the experimental dependence of the surface stress, τ, on the deformation, α, and the rate of deformation, $\dot{\alpha}$. Afterward, a suitable rheological model could be applied to describe the dependence, $\tau(\alpha,\dot{\alpha})$, and to extract the relevant rheological characteristics of the layer. In our analysis of the experimental data, we used the fact that at small surface deformations the surface stress was a linear function of the deformation and did not depend on $\dot{\alpha}$. From the slope of the respective line, we determined the surface dilatational elasticity.

2.4.4. Relaxation Times. The relaxation of the surface tension during the relaxation stage, after stepwise surface deformation, was analyzed to characterize the processes of surfactant adsorption (after expansion) and desorption (after compression). For the reasons explained in section 3.3.2, the experimental data were fitted with a biexponential function for relaxation after compression and with a triexponential function for relaxation after expansion:

$$\tau(t) = \sigma(t) - \sigma_e = \Delta\sigma_{1C}\exp\left(-\frac{t}{t_{1C}}\right) + \Delta\sigma_{2C}\exp\left(-\frac{t}{t_{2C}}\right) \quad (7)$$

$$\tau(t) = \sigma(t) - \sigma_e = \Delta\sigma_{1E}\exp\left(-\frac{t}{t_{1E}}\right) + \Delta\sigma_{2E}\exp\left(-\frac{t}{t_{2E}}\right) + \Delta\sigma_{3E}\exp\left(-\frac{t}{t_{3E}}\right) \quad (8)$$

Here, t_k (k = 1, 2, 3) represents the characteristic relaxation times, whereas $\Delta\sigma_k$ represents the related amplitudes of the relaxing stresses.

3. EXPERIMENTAL RESULTS AND DISCUSSION

Below we present and discuss the equilibrium surface tension isotherms (section 3.1), surface rheological properties (section 3.2), and relaxation processes after the stepwise deformation of the saponin layers, compared with the results for the dynamic surface tension of the saponin solutions (section 3.3).

3.1. Surface Tension Isotherms. The dependence of the equilibrium surface tension, σ_e, on the surfactant concentration, C_S, for two different saponin samples (QL Ultra and Supersap) is compared in Figure 2. No results are shown for saponin concentrations lower than 0.03 wt % (corresponding to ~2 μM) because the adsorption process was very slow and the results were irreproducible at such low concentrations. As expected, σ_e increased with the purity of the saponin samples: supersap solutions had systematically higher equilibrium surface tensions, by 1 to 2 mN/m, than those of QL Ultra. The experiments with QL 1000 showed that the surface tension for these samples was ~2.5 mN/m lower than that for Supersap (data not shown). Despite the different levels of purity, the critical micelle concentrations (cmc's) of all of the saponin extracts were approximately the same, cmc ≈ 0.025 wt %, which corresponds to 0.15 mM. This value is within the range found by Mitra and Dungan[23] for the cmc of saponin samples from different sources (varying from 0.013 to 0.074 wt %). Compared to other biosurfactants,[48] the saponins are among the most water-soluble, which leads to their relatively high cmc's and the high value of the equilibrium surface tension above the cmc, 38−40 mN/m (Figure 2). Compared to the typical synthetic nonionic surfactants, saponins also have relatively high cmc's: for example, the Tween family of surfactants has cmc's in the range of 10^{-3}−10^{-4} wt %, and Mirj surfactants have cmc's in the range of ~10^{-3}−10^{-2} wt %.[49,50]

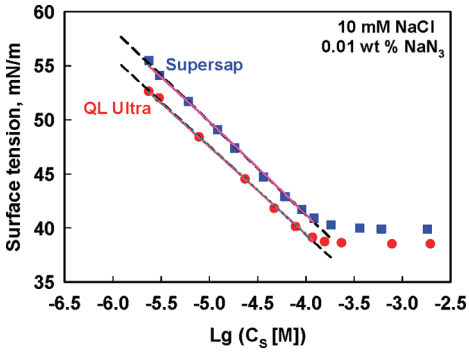

Figure 2. Equilibrium surface tension isotherms, measured by the Wilhelmy plate method at 25 °C, for two saponin samples: Supersap (blue squares) and QL Ultra (red circles). The solutions contained 10 mM NaCl and 0.01 wt % NaN_3. The lines below the cmc correspond to the best fits of the experimental data by Gibbs (dashed black lines), Volmer (continuous pink curve), and Langmuir (green dotted curves) adsorption models, which all give similarly good descriptions of the experimental data.

Below the cmc, the surface tension decreased linearly with the logarithm of saponin concentration, which is typical for nonionic surfactants.[50] Some authors describe saponins as nonionics,[32] but other authors note that they might behave as ionic surfactants as well because of the presence of carboxyl groups in the molecules.[23,34] To check for possible electrostatic effects, we added 150 mM NaCl to two solutions with concentrations below and above the cmc. The obtained experimental results showed that the surface tension of 0.013 wt % (below cmc) decreases from 40.1 to 39.1 mN/m for the QL Ultra sample and does not change when Supersap is used. The electrolyte effect was even less pronounced above the cmc, where the surface tension of the QL Ultra solution decreased by 0.3 mN/m, whereas no effect was seen for Supersap. Also, no effect of 1.2 mM $CaCl_2$ was observed for the solutions of Supersap, and a weak effect for the solutions of QL Ultra and QL 1000 was observed (data not shown). In contrast, for a typical ionic surfactant such as sodium dodecylsulphate (SDS), the difference in the values obtained at 10 and at 150 mM NaCl is larger than 4 mN/m.[51] Thus, we conclude that the studied *Quillaja* saponins behave as nonionic surfactants, which is in agreement with the results presented in ref 32.

Furthermore, the similar cmc values and the similar slopes of the isotherms for all saponin samples studied clearly show that the solution surface properties are governed by the saponin molecules whereas the other components in the nonpurified samples (proteins, polysaccharides, and phenols) have secondary importance.

To extract molecular information from the surface tension isotherms, we fitted the experimental data below the cmc with several adsorption isotherms:

3.1.1. Gibbs Adsorption Isotherm.[37,50−52]

$$\frac{d\sigma_e}{d\ln C_S} = -kT\Gamma \quad (9)$$

where k is the Boltzmann constant, T is the absolute temperature, C_S is the surfactant concentration in the bulk solution, and Γ is the surfactant adsorption (surface concentration).

3.1.2. Langmuir Adsorption and Surface Tension Isotherms.[37,50−52]

$$K_A C_S = \frac{\Gamma}{\Gamma_\infty - \Gamma} \quad (10a)$$

$$\sigma_e = \sigma_0 + kT\Gamma_\infty \ln\left(1 - \frac{\Gamma}{\Gamma_\infty}\right) \quad (10b)$$

Table 1. Values of the Adsorption Constant, K_A, Adsorption at the cmc, Γ_{cmc}, the Maximum Adsorption, Γ_∞, and the Corresponding Area Per Molecule, A_∞, as Determined from the Gibbs Adsorption Isotherm (Equation 9), Langmuir Adsorption Model (Equation 10), and Volmer Adsorption Model (Equation 11)

	Γ_{cmc}, 10^{18} m^{-2} (A_{cmc}, nm^2)			Γ_∞, 10^{18} m^{-2} (A_∞, nm^2)		K_A, 10^7 M^{-1}	
	Gibbs	Langmuir	Volmer	Langmuir	Volmer	Langmuir	Volmer
QL Ultra	0.87 ± 0.01 (1.16)	0.88 ± 0.01 (1.14)	0.91 ± 0.01 (1.10)	0.88 ± 0.01 (1.14)	1.02 ± 0.02 (0.98)	8.7 ± 1.5	19.5 ± 2
Supersap	0.91 ± 0.01 (1.11)	0.92 ± 0.01 (1.09)	0.95 ± 0.01 (1.05)	0.92 ± 0.01 (1.09)	1.08 ± 0.02 (0.92)	3.4 ± 0.5	7.0 ± 1.0

where K_A is the adsorption constant, σ_0 is the surface tension of the pure solvent (σ_0 = 72.0 mN/m for water at 25 °C), and Γ_∞ is the maximum adsorption in a complete adsorption monolayer.

3.1.3. Volmer Adsorption and Surface Tension Isotherms.[37,50−52].

$$K_A C_S = \frac{\Gamma}{\Gamma_\infty - \Gamma} \exp\left(\frac{\Gamma}{\Gamma_\infty - \Gamma}\right) \quad (11a)$$

$$\sigma_e = \sigma_0 - kT\Gamma_\infty \left(\frac{\Gamma}{\Gamma_\infty - \Gamma}\right) \quad (11b)$$

A nonlinear fit of the data was applied using two adjustable parameters for the Langmuir and Volmer adsorption isotherms: the adsorption constant, K_A, and the maximum adsorption, Γ_∞. The best fits, according to these three isotherms, are shown in Figure 2. One sees that all tested isotherms describe the experimental data very well, and from the fit alone, we cannot recognize which is more adequate. Note that the authors of ref 34 found that their results are best described by a Frumkin isotherm (corresponding to a modified Langmuir isotherm with included molecular interactions). However, our experimental data differ significantly from those presented in ref 34, which is probably due to the different saponin sources used.

The values of the parameters determined from the best fits are compared in Table 1. Along with the adsorption constant, K_A, the maximum adsorption, Γ_∞, and the adsorption at the cmc, Γ_{cmc}, the table also contains the calculated areas per molecule at the cmc, A_{cmc} = $1/\Gamma_{cmc}$, and in a dense monolayer, $A_\infty = 1/\Gamma_\infty$.

The areas per molecule at the cmc, determined by the three different isotherms (eqs 9−11), are almost the same for the two saponins studied: A_{cmc} = 1.13 ± 0.04 nm^2. Similar values of A_{cmc} (and of the related adsorption Γ_{cmc}), obtained from the three different theoretical models, are strong indication that these values are reliable and robust. The value of A_{cmc} is larger by 30% than the value of 0.83 nm^2, determined by Mitra and Dungan.[23] The difference is most probably related to the different producers of saponin extracts used in the two studies. Saponins are complex molecules and may undergo chemical changes (hydrolysis and structural isomerization) when treated differently.

The values of Γ_∞, determined by the Langmuir and Volmer models for given sample, are different, as expected, because the Langmuir model describes localized adsorption and the Volmer model describes nonlocalized adsorption.[50−54] The values of K_A obtained by the two models are also different, but we will not discuss this difference here because we do not know how accurate these values are. Note that both models neglect the possible attractive interactions between adsorbed molecules, and we are unable to determine these interactions from the experimental data.

Note that $A_\infty \approx 0.30$ nm^2 was determined in ref 34 and is much lower than that obtained by us (0.92 nm^2). To determine which of these values is realistic and what could be the reason for the observed difference, we determined the molecular dimensions of the saponin molecules by computer modeling (via the CambridgeSoft ChemOffice package). From the molecular model we found that the triterpenoid hydrophobic skeleton of *Quillaja* saponin occupies around 0.75 nm^2 in "lay-on" orientation on the solution surface and around 0.26 nm^2 in "end-on" orientation (Figure 3). The hydrophilic chains slightly increase the cross section of the molecule when properly oriented with respect to the hydrophobic part. Comparing these values to the area per molecule, as determined from the adsorption isotherms (Table 1), we conclude that the saponin molecules are most probably oriented in the lay-on configuration in our experiments (Figure 3A). The smaller value of A_∞ determined in ref 34 would imply the end-on configuration of the molecules in the respective experiments. A more detailed analysis, which is beyond the scope of the current study, is needed to establish whether this difference is due to the specific saponin batches used in these studies or to the different procedures for data analysis. On the basis of the slope (below the cmc) of the experimental surface tension isotherm measured by us and its rigorous interpretation by the model-free Gibbs adsorption isotherm (eq 9), we can be sure that the area per molecule in our studies is around 1 nm^2.

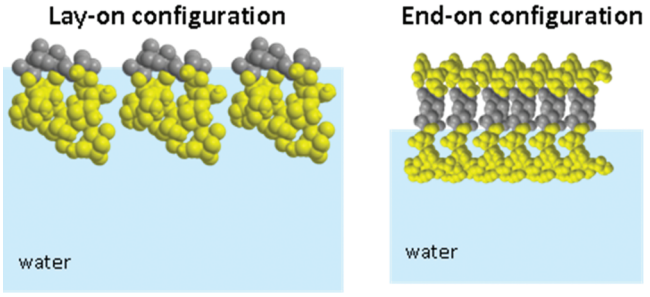

Figure 3. Schematic presentation of two possible orientations of the saponin molecules in the adsorption layer. The dark-gray regions represent the hydrophobic triterpenoid rings, and the yellow regions represent the hydrophilic sugar residues in the molecule. The lay-on orientation corresponds to an ∼1 nm^2 area per molecule, whereas the end-on orientation corresponds to ∼0.3 nm^2.

Using the best-fit parameters presented in Table 1, we calculated the adsorption, $\Gamma(C_S)$, surface coverage, $\theta(C_S) = \Gamma/\Gamma_\infty$, and Gibbs elasticity, $E_G = -d\sigma/d \ln \Gamma$, for the two saponin samples studied, Supersap and QL Ultra. Each of the models used predicts similar dependencies for the two saponin samples, with the adsorption for Supersap being slightly lower than that for QL Ultra. As a result, the surface coverage, $\theta(C_S)$, and the elasticity, $E_G(C_S)$, are also slightly lower for Supersap. Despite these small differences, one should emphasize that the results for Supersap and QL Ultra are very similar to each other, which is another proof that the surface properties of the nonpurified saponin extracts are governed by the saponin molecules.

In Figure 4, we plot the Gibbs elasticity as a function of saponin concentration, as calculated by the Langmuir and Volmer models for the two saponin samples. One sees that the two theoretical models predict very different Gibbs elasticities. According to the Langmuir model, the saponin adsorption layers are almost complete at the cmc, and as a result, this model predicts a very high Gibbs elasticity of ∼2 × 10^4 mN/m at the cmc. In contrast, the Volmer model predicts surface coverage $\Gamma_{cmc}/\Gamma_\infty \approx 88\%$ and $E_G \approx 260$ mN/m around the cmc. The results for the

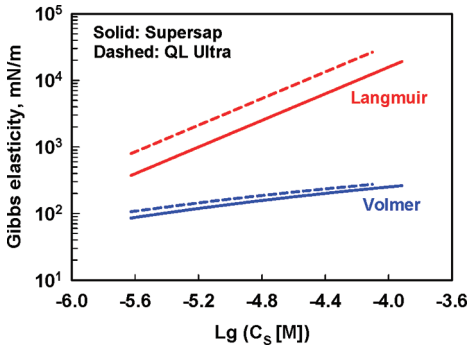

Figure 4. Calculated Gibbs elasticity, E_G, for Supersap (solid curves) and QL Ultra (dashed curves) using the Langmuir (red curves) and Volmer (blue curves) adsorption models.

two saponin samples are very similar, as already explained. Because the purified Supersap batch better represents the *Quillaja* saponins with the least effect of the impurities present in the original extract, below we present and discuss the results primarily for Supersap.

It is generally accepted that the Volmer model is more adequate for the description of fluid surfaces with mobile adsorbed molecules, whereas the Langmuir model is considered to be more appropriate for the description of localized adsorption on solid surfaces.[54,55] It is not obvious in advance which of these models is more appropriate for the description of saponin layers, which have a high surface elasticity (section 3.2) possibly reflecting a solidified adsorption layer. One way to test the adequacy of these two models is to compare their predictions for the Gibbs elasticity and for the surface relaxation time, t_r, with the experimental data for these quantities.[54] Such a comparison and its discussion are presented in the following two sections.

3.2. Surface Rheological Properties upon Surface Deformation. Several complementary experimental techniques were used to characterize the surface rheological properties (surface elasticity and viscosity) of the saponin adsorption layers.

3.2.1. Oscillatory Deformation in the Langmuir Trough. These experiments were performed with solutions containing 0.1 wt % (0.61 mM) Supersap saponin by applying two different orientations of the Wilhelmy plate: perpendicular and parallel to the moving barriers. For solidlike adsorption layers with high surface elasticity, such measurements allow one to extract information for both the shear and dilatational elastic moduli of the layers.[46,47]

Typical oscillation curves for the surface area, A, and the surface pressure, $\Pi = (\sigma_0 - \sigma)$, are shown in Figure 5A. The shape of the area oscillations was of a triangular type, the period of oscillation was 9.5 s, and two amplitudes of deformation (4 and 6%) are shown in Figure 5A. The response of the surface pressure was also triangular and was in phase with the area oscillations, which indicates the elastic response of the layer under these conditions.

Figure 5B represents the same data as the surface stress, τ, versus area deformation, α. One sees that τ is a linear function of α and that the surface stress does not depend noticeably on the rate of surface deformation, which confirms that the saponin adsorption layer behaves as a purely elastic body in this deformation regime. Such elastic behavior was detected with both parallel and perpendicular orientations of the Wilhelmy plate. From the slopes of the experimental dependencies in these two configurations, we determined $\tau_{\parallel}/\alpha = 285 \pm 5$ mN/m and $\tau_{\perp}/\alpha = 233 \pm 10$ mN/m. By introducing these values into eqs 6, we calculated the surface dilatational elastic modulus, $K = 259 \pm 15$ mN/m, and the surface shear elastic modulus, $\mu = 26 \pm 15$ mN/m, of the layers.

Note that the measured surface dilatational elasticity is very close to the Gibbs elasticity at the cmc, as predicted by the Volmer model (262 mN/m), and differs significantly from that predicted by the Langmuir model (18 600 mN/m). This very good agreement with the Volmer model implies that this model is more adequate for the description of the saponin layers and that related parameters $A_\infty \approx 0.92$ nm^2, $\Gamma_{cmc}/\Gamma_\infty \approx 88\%$, and $K_A \approx 7 \times 10^7$ M^{-1} are more reliable.

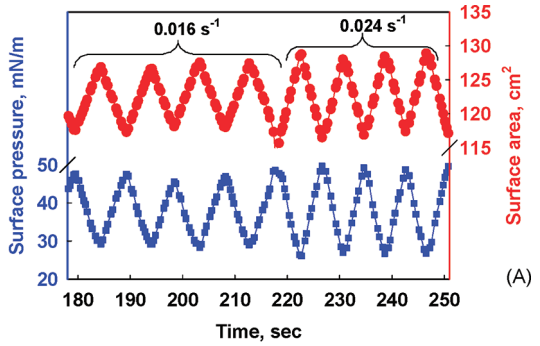

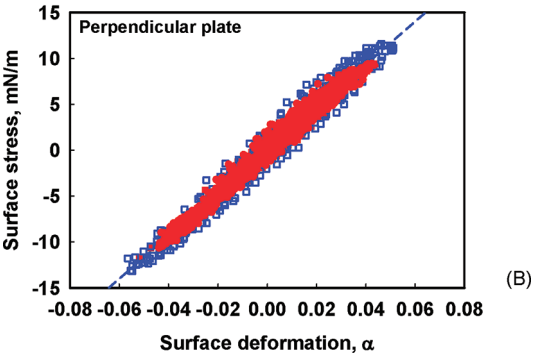

Figure 5. (A) Surface pressure, $\Pi(t)$, (left axis) during consecutive expansions and compressions of the area (right axis) at two different oscillation rates (as indicated) of the saponin adsorption layer formed from a 0.1 wt % Supersap solution. (B) Surface stress, τ, as a function of surface deformation, α, for four experimental runs made at two different deformation rates of 0.016 s^{-1} (red symbols) and 0.024 s^{-1} (blue symbols). The measurement was made with a Wilhelmy plate oriented perpendicular to the direction of barrier movement in the Langmuir trough.

Thus, we conclude from these experiments that at a surface deformation of below 6% and a rate of deformation of between 0.016 and 0.024 s^{-1} the saponin adsorption layers behave purely elastically with a surface dilatational elasticity of ~260 mN/m, in agreement with the Volmer model. Under these conditions, the *Quillaja* saponin behaved as an insoluble surfactant (i.e., the adsorption/desorption rate was lower compared to the rate of area deformation).

3.2.2. Layer Expansion/Compression at a Constant Rate in the Langmuir Trough. In this type of experiment, consecutive expansions and compressions are applied, with each of them followed by a relaxation period. In this section, we describe the results from the deformation periods only. The results from the relaxation periods are presented in section 3.3.

These experiments were performed in a Langmuir trough with 0.1 wt % solutions of Supersap at two orientations of the Wilhelmy plate (perpendicular and parallel). The major differences between these experiments and those described in section 3.2.1 are (1) The surface layer has time to relax before the next deformation and (2) the total surface deformation in these experiments is 2 times larger than the surface deformation in the oscillation experiments, viz., 12%. The rates of oscillation were fixed at 0.016 and 0.024 s^{-1} as in the previous experiments.

Typical experimental results from several consecutive expansions and compressions of the layer, along with the resulting change in the surface

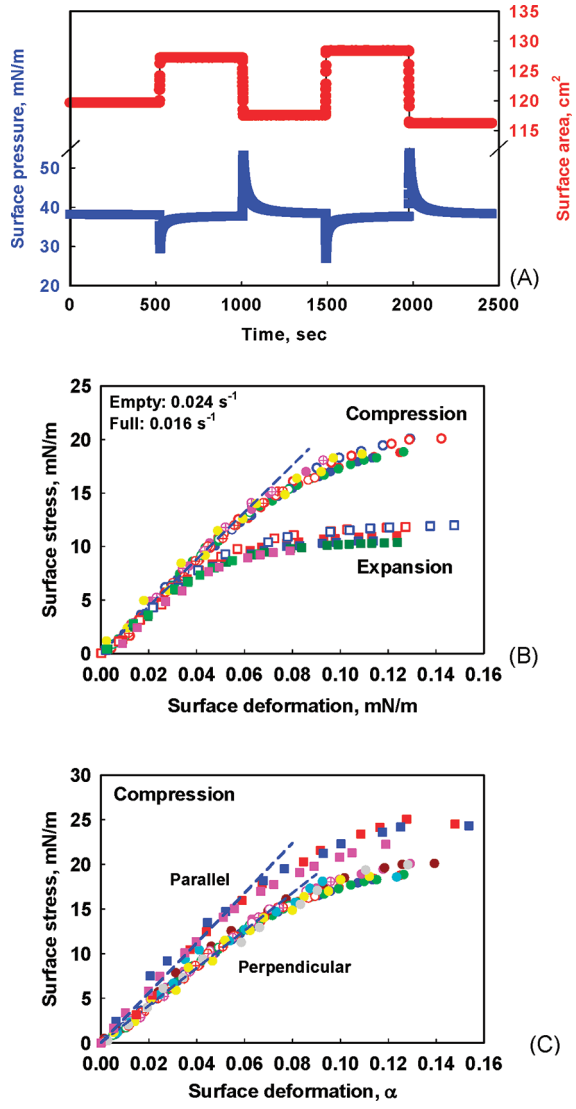

Figure 6. Experimental results from deformation−relaxation measurements with a 0.1 wt % Supresap solution in the Langmuir trough. (A) Surface pressure, $\Pi = (\sigma_0 - \sigma)$, (blue curve, left axis) during consecutive expansions and compressions of the area (red curve, right axis). (B) Absolute value of the surface stress, τ, measured by the perpendicular orientation of the plate as a function of the surface deformation, α, during expansion (squares) and compression (circles) at two different rates of deformation, 0.016 s^{-1} (solid symbols) and 0.024 s^{-1} (open symbols). (C) Absolute value of the surface stress vs surface deformation, α, for compression, as measured by the parallel orientation of the plate (squares) and the perpendicular orientation of the plate (circles).

pressure, are shown in Figure 6A. Figure 6B presents the absolute value of the surface stress, τ, as a function of the surface deformation for both expansion and compression. One sees that at low surface deformation (up to 5%) there is no significant difference between compression and expansion—the saponin layer behaves as purely elastic, and the surface stress is a linear function of deformation and does not depend on the rate of deformation. As in the case of the oscillatory experiments, we observed a noticeable (though not a very large) difference in the slopes of the curves for the two orientations of the measuring plate (Figure 6C). From these slopes, we determined $\tau_{\parallel}/\alpha = 280 \pm 10$ mN/m and $\tau_{\perp}/\alpha = 220 \pm 10$ mN/m, which is in very good agreement with the results obtained from the oscillatory experiments. Thus, we confirm that the saponin layers behave as an elastic body up to deformations of 5%, with a very high dilatational elastic modulus and a low shear elastic modulus.

However, when the surface deformation increases to above 5%, a significant difference in the shape of the curves, $\tau(\alpha)$, is observed for compression and expansion (Figure 6B). At large surface deformation, the surface stress upon compression is higher than the stress upon expansion, which indicates a slower layer relaxation upon compression as compared to the relaxation after expansion. One may expect that at such a large expansion the adsorption layer becomes sufficiently dilute so that fast molecular adsorption is triggered from the adjacent bulk phase.

A qualitative analysis of the shape of the curves and direct numerical calculations showed that these experimental data cannot be described by a Maxwell or Kelvin−Voigt rheological model. Let us illustrate just one of the arguments leading to this conclusion. The Maxwell model predicts that the plateau in the curve $\tau(\alpha)$ for large deformations is equal to $\eta\dot{\alpha}$, which implies that the ratio of the plateau values for the two rates of deformations used in our experiments (0.016 and 0.024 s^{-1}) should be equal to the ratio of these rates (i.e., 1.5). However, the data presented in Figure 6B give a values of less than 1.1 for this ratio, which is in obvious contradiction with the Maxwell model. Therefore, more complicated rheological models are currently constructed and tested for a quantitative description of these experimental data.

From this series of experiments, we can conclude that the saponin adsorption layers behave as an elastic body during deformation of up to 5%, with a surface dilatational elasticity of around 260−280 mN/m. Above this deformation, a significant difference is observed in the $\tau(\alpha)$ curves for compression and expansion. The surface stress upon expansion is lower compared to that for compression, which implies faster saponin adsorption as compared to desorption.

3.2.3. Oscillatory Surface Deformation Using the Spherical Drop Method. Experiments with spherical drops were performed with 0.1 wt % Supersap solutions. A sinusoidal deformation of the surface area was applied, and the oscillations of the surface tension were measured by capillary pressure tensiometry.[45] These experiments were performed at a maximum surface deformation of 2.6%. This method allows one to determine the rheological properties of the adsorption layers as a function of the oscillation period. To compare the results from the Langmuir trough and the oscillating drop method, we included here measurements for a 10 s period, which corresponds to the same maximum rate of surface deformation, 0.016 s^{-1}, as that applied in the Langmuir trough.

The obtained results for the surface moduli, E' and E'', as a function of the oscillation period, are shown in Figure 7. One sees that the surface elastic modulus is much higher than the loss modulus for all oscillation periods studied. These results demonstrate again that, for small deformations, the saponin layers behave as a predominantly elastic body even for a very long period of oscillation, T = 50 s. We observed a slight decrease in the surface elastic modulus from 310 to 270 mN/m upon increasing the period of oscillation from 10 to 50 s. In parallel, we observed that the surface loss modulus increased slightly up to 25 mN/m at an oscillation period of around 20 s and remained constant at longer periods. The latter result indicates the occurrence of a slow relaxation process with a characteristic time of 10−20 s. (See section 3.3 for a more detailed discussion of the relaxation behavior of the layers.)

A direct comparison of the results obtained by the oscillating spherical drop method (OSDM) and Langmuir trough can be made at 10 s of oscillation. The surface elastic modulus measured with OSDM is ∼310 ± 20 mN/m, and the modulus measured in the Langmuir trough is 260 ± 20 mN/m. The most probable reason for this small discrepancy (∼15%) could be slight deviations of the drop from its spherical shape during oscillations, a possibility that is suggested by the results and discussion presented in section 3.2.5 (due to oscillations of the deformed drop). To some extent, this difference could also be due to the different surface deformations used in the two methods, 6% in the Langmuir trough and 2.6% in the OSDM method.

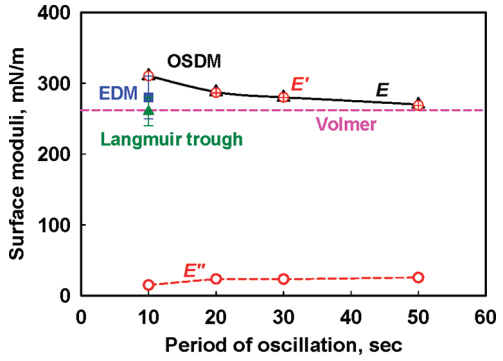

Figure 7. Total surface modulus, E (black full triangles connected by solid line), elastic modulus, E' (red crossed circles), and viscous modulus, E'' (red empty circles connected by a dashed line), as functions of the oscillation period, measured by the oscillating spherical drop method at a 2.6% deformation amplitude with a 0.1 wt % Supersap solution (in the presence of 10 mM NaCl and 0.01 wt % NaN_3). The pink horizontal dashed line represents the Gibbs elasticity calculated by means of the Volmer equation. The blue square is the result obtained by the expanding drop method, and the green triangle is the result from experiments in the Langmuir trough.

3.2.4. Expansion of Spherical Drops. In these experiments, we measured the surface stress as a function of surface deformation for spherical drops expanded at a constant rate of 0.04 s^{-1}. Details of the experimental procedure can be found in ref 44. The obtained results for the 0.1 wt % Supresap solution are presented in Figure S1 in the Supporting Information. The experimental data are somewhat scattered; nevertheless, we can determine with reasonable accuracy the surface elasticity from the slope of the experimental line, which was found to be 280 ± 30 mN/m. This value is in agreement with those obtained by the other methods discussed so far and with the prediction of the Volmer adsorption model.

3.2.5. Oscillation of a Deformed Drop with Drop-Shape Analysis (ODDM-DSA). In these experiments, sinusoidal oscillations of a drop deformed by gravity are performed, and the surface tension is measured from the drop shape by the fit with the Laplace equation of capillarity. Note that in the experiments with spherical drops (OSDM) the surface tension was determined by a direct measurement of the capillary pressure with a pressure transducer (i.e., these are two conceptually different experimental methods, though both rely on the Laplace equation for data interpretation).

A series of experiments were performed at different periods of oscillations and deformations, and the obtained results are summarized in Figure 8. Again, we found that the saponin layers behave as an elastic body (loss modulus ≈ 0). However, the measured values of the surface modulus were two and a half times lower than those measured with all other methods used (Langmuir trough, oscillating spherical drop, and expanding spherical drop). The experimental results showed that the surface modulus did not depend significantly on the surface deformation up to 8% (Figure 8B). There was some decrease in the surface modulus from 110 to 95 mN/m with the increase of the oscillation period, but this effect was also relatively small.

To determine whether the values measured by the oscillating deformed drop method (ODDM-DSA) are affected by the shape of the oscillations applied, we performed additional experiments with triangle oscillations of the drop surface. In these experiments, we again measured the surface modulus to be around 115 ± 15 mN/m, as in the case of the sinusoidal oscillation. Thus, we conclude that the ODDM-DSA gives substantially lower values for the surface elasticity of the adsorption layers, as compared to the other methods used. Note that all experimental methods gave virtually the same values for the equilibrium

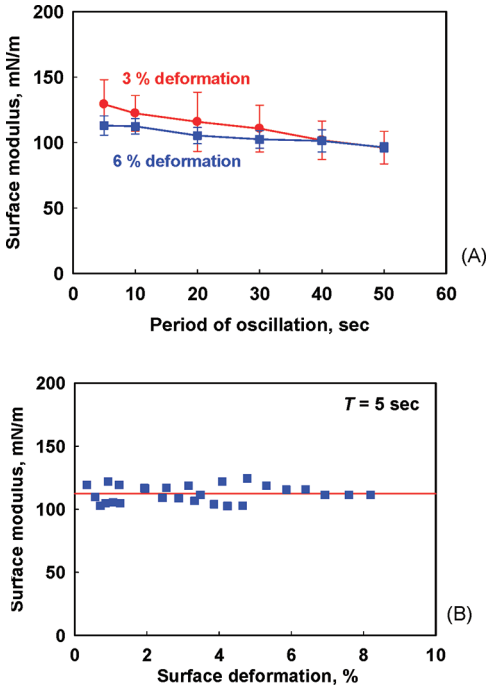

Figure 8. Total surface modulus, E, as a function of (A) the period of oscillation at two different oscillation amplitudes and (B) the surface deformation at a 5 s period of oscillation as measured by the oscillating deformed drop method (ODDM-DSA) with 0.1 wt % Supersap + 10 mM NaCl + 0.01 wt % NaN_3 at 25 °C.

Figure 9. Image of a pendant drop from a 0.1 wt % saponin solution after fast surface compression with α = 12%. The wrinkles in the region of the elongated drop neck indicate the compressed nonhomogeneous adsorption layer.

surface tension of the solutions; that is, a discrepancy is observed only in the dynamic measurements.

By analyzing the possible sources of errors in the various methods, we found most problematic the assumption that the deformation of the drop surface is isotropic in the ODDM method. Indeed, when we applied a fast, relatively large compression of the drop, we saw the formation of vertical surface wrinkles in the region of the elongated neck of the drop. (See the image in Figure 9 taken at 12% surface compression.) If the compressed drop was left to relax at constant volume, then the wrinkles slowly disappeared and the surface tension relaxed to its equilibrium value.

dx.doi.org/10.1021/la202860u |*Langmuir* 2011, 27, 12486–12498

These wrinkles demonstrate two important phenomena, relevant to our discussion. First, the wrinkles are a clear manifestation of the unusual rheological properties of such highly elastic layers because they indicate a very low surface tension, leading to the spontaneous buckling of the adsorption layer. Previously, similar wrinkles were reported with insoluble monolayers of solid particles, lipids, and some specific proteins.[33,56−58]

Second, the position and vertical orientation of the wrinkles indicate that the surface deformation is nonhomogeneous along the drop surface —the compression is largest in the neck of the drop (where the wrinkles appear during neck shrinking) and smallest at the drop apex (where no wrinkles are seen). In addition, the vertical orientation of the wrinkle indicates a nonisotropic surface deformation. Such a nonisotropic deformation could occur because of the small but non-negligible shear elasticity of the saponin adsorption layer, as explained in section 3.2.1, and/or because of the high surface shear viscosity.

Let us note also that much larger drops (typical volume of 15 mm^3 and surface area of 28 mm^2) are used in the ODDM-DSA method as compared to the OSDM (typical volume of 3 mm^3 and surface area of 8 mm^2) in order to have a sufficient deformation of the drop shape by gravity. This difference suggests that the shape of the larger deformed drops in the ODDM-DSA method could be affected more significantly by surface nonhomogeneities, in comparison with the shape of the smaller spherical drops.

Nonhomogeneous deformations of elastic layers, such as those shown in Figure 9, create surfaces that do not necessarily comply with the main assumption implemented in the ODDM-DSA method, namely, that the surface is fluid and homogeneous, so the Laplace equation of capillarity could describe the entire drop with a single value of the surface tension (as the only fit parameter). Instead, the dynamic shape of the drop could depend on other parameters, such as the shear surface elasticity and viscosity, which makes the method inapplicable for an accurate determination of the surface moduli. This latter explanation was also supported by the numerical fit error calculated by the instrument in the process of image analysis − the fit errors of the oscillating drops were systematically 1 order of magnitude larger than those for the equilibrium pendant drops in the case of saponin layers. No such difference in the fit errors was seen for conventional LMW surfactants.

Note that only the ODDM-DSA method relies on the use of the drop deformation for calculating the surface tension. It is well known that small deviations in the drop shape from the equilibrium shape lead to large errors in the values of the surface tension, as determined by this method.[45] The other methods rely on more robust procedures, such as measuring the total weight of the meniscus attached to the Wilhelmy plate (in the Langmuir trough) or measuring the pressure jump across an approximately spherical interface (for the OSDM and the expanding drop method). Therefore, these methods are based on measuring cumulative or average quantities and are therefore expected to be less affected by small local variations in the surface properties as compared to those determined by the ODDM-DSA method.

In concluding this analysis, we claim that the oscillating drop method, with deformed by gravity pendant drops, has specific problems when applied to the characterization of the dynamic properties of highly elastic adsorption layers. For such layers, a Langmuir trough with two movable barriers and oscillating spherical drops are the preferred methods because both involve a better defined deformation of the surface—unidirectional in the first case and an almost homogeneous affine deformation in the second case. It is worth stressing explicitly that without other methods of comparison one could easily accept the values measured by the ODDM-DSA method as correct because they seem realistic and there is no any obvious warning sign in the obtained results (except for the larger fit error).

From all of the results described so far, we can conclude the following: (1) The saponin layers behave as an elastic body up to 5% deformation with a surface elasticity of 280 ± 30 mN/m, which is in a good agreement with the predictions of the Volmer model. (2) At small deformations (up to 5%), the measured surface elasticity does not significantly depend on the oscillation period in the range of 10 to 50 s, which means that for small deformations the relaxation characteristic time is rather long. (3) When the deformation becomes larger than 5% upon expansion and larger than 9% upon compression, a fast relaxation process is triggered with a characteristic time of several seconds. (4) The oscillating deformed drop method (ODDM-DSA) is not appropriate for determining the surface rheological properties of layers with a high surface elasticity because it gives inaccurate results.

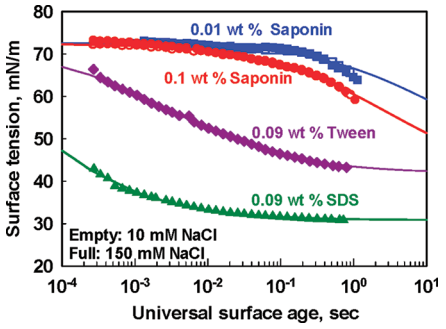

Figure 10. Dynamic surface tension as a function of universal surface age measured by the MBPM for Supersap solutions (red and blue symbols) with concentrations indicated in the figure and for 0.09 wt % SDS and 0.09 wt % Tween 20 solutions shown for comparison. The solid symbols are for solutions containing 150 mM NaCl, whereas the open symbols are for solutions with 10 mM NaCl. The curves are the best fits of the experimental data by eq 12.

3.3. Relaxation of Perturbed Saponin Layers. In this section, we determine the characteristic relaxation times of perturbed saponin adsorption layers. First, we present and discuss the results for the dynamic surface tension of the solutions measured by MBPM (for short and intermediate times) and by the Wilhelmy plate (for long times). Next, the results from the relaxation part of the stress−relaxation curves obtained in the Langmuir trough (Figure 6A) are described and analyzed.

3.3.1. Dynamic Surface Tension. We measured by MBPM the dynamic surface tension of solutions containing 0.01 and 0.1 wt % Supersap. The lower concentration is below cmc ≈ 0.025 wt %, whereas the higher concentration is above the cmc. The obtained results are shown in Figure 10 and are compared with the results for two typical low-molecular-weight (LMW) surfactants—nonionic Tween 20 and ionic SDS (both with concentrations of 0.09 wt %). The experiments with LMW surfactants are performed at 150 mM NaCl to screen the electrostatic adsorption barriers.[51] Experiments with saponin solutions are performed at electrolyte concentrations of 10 and 150 mM NaCl.

One sees from Figure 10 that the dynamic surface tension of the two saponin solutions decreases much more slowly than that of Tween and SDS solutions, despite the similar weight concentrations of all surfactants. One possible explanation for the observed different characteristic times of the studied surfactants could be the different monomer concentrations in the solutions, which would imply different diffusion fluxes toward the freshly formed surface. However, when comparing the cmc values of the surfactants, we estimate that the saponin monomers (0.15 mM) have a concentration that is 2 orders of magnitude higher than that of Tween monomers (1.1 μM)[59] and 1 order of magnitude lower than that of SDS (1 mM).[51] Therefore, the monomer concentrations can explain in part the fastest $\sigma(t)$ decrease with SDS; however, it cannot explain the slower decrease with saponin, as compared to that of Tween 20.

Note that the results with saponin solutions containing 10 and 150 mM NaCl coincide. Similar results were obtained in the presence

of 1.2 mM $CaCl_2$ and 10 mM NaCl (data not shown). This independence of the electrolyte concentration reinforces the conclusion that saponin adsorbs as a nonionic surfactant without electrostatic effects present.

To make an approximate estimate of the characteristic adsorption time for the solutions studied, we processed the MBPM data in the following way: (1) We plotted the surface tension as a function of the so-called "universal" surface age, $t_u = t_{age}/37$, by applying the correction factor found in ref 60 for diffusion-controlled adsorption. (2) We fitted the experimental results using the asymptotic equation, which is valid for not-too-small values of the surface age:[60]

$$\sigma = \sigma_e + \frac{s_\sigma}{a_\sigma} \frac{1}{1 + \sqrt{t_u/a_\sigma{}^2}} \tag{12}$$

where $\sigma(t)$ is the dynamic surface tension, σ_e is the equilibrium surface tension, t_u is the universal surface age, and s_σ and a_σ are the two fit parameters ($a_\sigma{}^2$ represents the characteristic time of adsorption).

The term "universal age", t_u, was introduced in ref 60; it is the surface age that would have the same instantaneous surface tension as that measured in the instrument at time t_{age} if the surface was not expanding during the experiment. Therefore, the correction factor used to calculate t_u from t_{age} accounts for the large surface expansion (the surface area increases by several orders of magnitude) and the related convective mass transfer of surfactant toward the interface, which are inherent to the MBPM. It was shown in ref 60 that this numerical factor is specific for the MBPM instrument used, and for the BP2 device used in our study, it is equal to 37. In other words, the surfactant adsorption would be 37 times faster for the same surfactant solution if the surface was not greatly expanding during the MBPM measurements. In all further considerations, we plot and discuss the experimental data in terms of the universal age, t_u, because this allows one to compare the kinetic results from the MBPM with those obtained by other methods in which small surface perturbations are applied.

The curves in Figure 10 represent the best fits to eq 12 of the experimental data for $\sigma(t)$. A reasonably good description of all experimental data is seen in Figure 10, and from these fits, we determined the characteristic adsorption times for the various surfactants: 3 s for 0.1 wt % saponin, 3.1 ms for Tween 20, and 27 μs for SDS. Therefore, the characteristic adsorption time for saponin is 3 orders of magnitude longer than that for Tween 20 and 5 orders of magnitude longer that that for SDS. With the decrease in the saponin concentration from 0.1 to 0.01 wt %, the characteristic adsorption time increases from 3 to 10 s.

Theoretically, the characteristic adsorption times for diffusion-controlled adsorption from the monomer solution (below and at the cmc) can be estimated by the following expression:[52]

$$t_\sigma = \frac{1}{D}\left(\frac{\Gamma^2 kT}{C_S E_G}\right)^2 \tag{13}$$

With the parameters of the Volmer adsorption isotherm from Table 1 and an estimated diffusion coefficient of $D = 2 \times 10^{-10}$ m^2/s, we calculate 1.9 ms for a 0.01 wt % saponin solution and 8.2 μs for the saponin solutions at cmc. Thus, we conclude that the actual saponin adsorption is 4 orders of magnitude slower than that predicted theoretically for diffusion control, which means that saponin adsorption is barrier-controlled.

A relevant question is whether the MBPM data, obtained with saponin solutions, are significantly affected by the possible surface nonhomogeneities, as discussed in section 3.2.5, in relation to the ODDM-DSA method. We do not expect such complications because one applies rapid surface expansion only in the MBPM and therefore the adsorption saponin layers are very dilute when the maximum pressure is measured by this method, as evidenced by the high dynamic surface tensions of the saponin solutions in Figure 10. One could expect that the specific phenomena discussed in section 3.2.5 are more typical of dense adsorption layers in which the molecules are compressed and have high barriers to desorption, especially when surface compression is applied. In addition, measurements made by pressure with almost spherical bubbles in the MBPM are expected to be less affected by the discussed problems because this method does not rely on analyzing small variations in the drop shape, as is the case with the ODDM-DSA method. In concludsion, we do not expect the MBPM data to be affected significantly by the complications discussed in section 3.2.5.

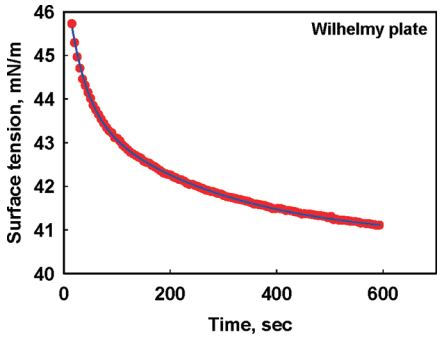

Figure 11. Surface tension as a function of time for 0.1 wt % Supersap (+ 10 mM NaCl + 0.01 wt % NaN_3) as measured by the Wilhelmy plate method. The red points are experimental data, whereas the blue curve is the best fit with the biexponential function.

In another series of experiments, we measured the surface tension of saponin solutions by the Wilhelmy plate method, which allows us to study the long-term kinetics of adsorption (Figure 11). The experimental data were fitted very well by two exponents (eq 7). From the best fit of the experimental data, we determined the equilibrium surface tension and two additional characteristic times of saponin adsorption (beside that determined by the MBPM), which are around 30 ± 10 and 250 ± 50 s for the 0.1 wt % Supersap solution (Figure 11).

The main conclusions from these experiments are the following: (1) The saponin adsorption is barrier-controlled. (2) There are three well-separated characteristic times of adsorption: the shortest time, ~3 s, corresponds to the actual molecular adsorption and two additional slower processes are observed (most probably related to the slow rearrangement of the molecules in the adsorption layer) with characteristic times of ~30 and ~250 s.

3.3.2. Relaxation Processes after Deformation in the Langmuir Trough. In this section, we analyze the relaxation part of the curves obtained in the deformation−relaxation experiments (Figure 6A). As shown in section 3.2.2, there is a large difference in the stresses registered after compression and expansion (Figure 6B). Therefore, the stress relaxes from different initial values after periods of compression and expansion performed up to the same total deformation.

Experimental data for the absolute value of the relaxing surface stress are presented in Figure 12. One sees a significant difference in the evolution of the relaxing stresses after compression and expansion. The surface stress after compression is much higher than the stress after expansion during the first 10 s; however, the reverse trend is observed after 50 s. Furthermore, the surface stress becomes zero for compressed layers after 200 s, whereas the stress in the expanded layer is still detectable, ~0.2 mN/m, and slowly decreases even after 300 s.

To analyze these data, we fitted them with three relaxation times for expanded layers (eq 8) and with two relaxation times for compressed layers (eq 7). The obtained results from the various types of experiments are summarized in Table 2.

One sees that the fast relaxation time after expansion is 2.8 s, which practically coincides with the characteristic time for saponin adsorption,

as determined from the MBPM (Figure 10). Note that this relaxation processes starts in the expansion period, when the surface deformation exceeds 5%. Therefore, we can conclude that this first characteristic time after expansion is related to the actual adsorption of new molecules from the bulk solution to the expanded adsorption layer, when the surface deformation is larger than 5%. The surface stress, which relaxes with this characteristic time, is ~5 mN/m in the experiments, in which the shear rate is 0.016 s^{-1}, and 6.3 mN/m when the rate of expansion is 0.024 s^{-1}. This stress depends on the rate of deformation but does not depend on the final deformation.

The second and third relaxation times are ~20 and 200 s, which are also in a reasonable agreement with the characteristic times measured by the Wilhelmy plate method. The stresses, which relax with these characteristic times, depend on the expansion amplitude but do not depend on the rate of deformation (just the opposite of the fastest relaxation mode) (Table 2). These dependences indicate that the slow relaxation processes are related to the rearrangement of the saponin molecules in the adsorption layer.

The relaxation parameters for compressed layers are also presented in Table 2, and they are very different from those for expanded layers. The first relaxation time for the compressed layer is much longer (7.2 vs 2.8 s); that is, the fastest relaxation process after compression is slower than the fastest relaxation processes after expansion (i.e., the desorption of saponin molecules is even slower than their adsorption). Interestingly, the fastest desorption time decreases from 11 to 7 s when the surface compression increases from 6 to 12%. A similar increase is observed for the intermediate relaxation process as well, from 36 to 62 s. Note that, in contrast, neither of the relaxation times for the expanded layers depend significantly on the deformation and on the rate of deformation. For compressed layers, however, a significant effect of deformation is observed, which shows that the system is not linear for the deformations applied.

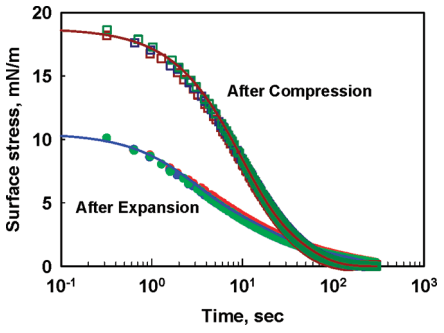

Figure 12. Absolute value of the surface stress as a function of time during relaxation after expansion (circles) and compression (squares) up to a surface deformation of 12% at a surface deformation rate of 0.016 s^{-1}. The experiments are performed with 0.1 wt % Supersap (+ 10 mM NaCl + 0.01 wt % NaN_3) in a Langmuir trough. The blue curve is the best fit by eq 8, and the dark red curve is the best fit by eq 7.

4. CONCLUSIONS

Quillaja saponins are natural surfactants that have attracted considerable interest in recent years because of their bioactivity and their remarkable properties as foamers and emulsifiers. In this article, we present a systematic characterization of the major surface properties of highly purified *Quillaja* saponins. The main results can be summarized as follows:

- The surface properties of nonpurified saponin extracts are governed by the saponin molecules, whereas the other extracted components (polyphenols, proteins, and polysaccharides) have secondary importance.
- The purified *Quillaja* saponins behave as nonionic surfactants with a relatively high cmc (0.025 wt %). The saponin adsorption isotherm is described well by the Volmer equation with $A_{cmc} \approx 1.05$ nm^2, $A_\infty \approx 0.92$ nm^2, and $K_A \approx 7.0 \times 10^7$ M^{-1}. This area per molecule corresponds to the lay-on configuration of the saponin molecules in the adsorption layer.
- Under small deformations (up to 5%), the saponin adsorption layers behave as 2D elastic bodies with a surface dilatational elasticity of 280 ± 30 mN/m. This value agrees well with the Gibbs elasticity, as calculated by the Volmer equation of state (260 mN/m). The surface shear elasticity of saponin adsorption layers is much lower, 26 ± 15 mN/m.
- At deformations larger than 9% upon compression and 5% upon expansion, molecular desorption/adsorption processes are triggered. The saponin adsorption is barrier-controlled and relatively slow (characteristic time ≈ 3 s). The saponin desorption is even slower (characteristic time ≈ 7 s).
- The relaxation processes after compression and expansion are complex and involve several slow relaxation times (up to 200 s), corresponding to slow molecular rearrangements in the adsorption layer.
- The oscillating deformed drop method with drop-shape analysis (ODDM-DSA) was shown to provide a 2.5 times lower surface modulus for the saponin system studied here as compared to the other methods used. The reasons for this discrepancy are discussed, and a plausible explanation is provided.

Table 2. Results from the Best Fit of the Experimental Data by Equation 8 for Expanded Layers and by Equation 7 for Compressed Layers[a]

	after expansion		after compression	
parameter	α = 0.12	α = 0.06	α = 0.12	α = 0.06
$\Delta\sigma_1$, mN/m (at 0.024 s^{-1})	5.2 ± 0.6 (6.3 ± 0.2)	5.0 ± 0.1 (6.4 ± 0.2)	11.2 ± 0.8 (13.0 ± 0.2)	10 ± 1
t_{r_1}, s	2.8 ± 0.5	2.7 ± 0.2	7.2 ± 0.8	11 ± 1
$\Delta\sigma_2$, mN/m	3.7 ± 0.2	3.2 ± 0.1	7.2 ± 0.9	5.1 ± 0.3
t_{r_2}, s	19 ± 2	19 ± 1	36 ± 4	62 ± 14
$\Delta\sigma_3$, mN/m	1.8 ± 0.2	1.3 ± 0.1		
t_{r_3}, s	180 ± 40	180 ± 20		

[a] α is the maximum surface deformation in the deformation period, preceding the relaxation. The experiments are performed at two rates of deformation, 0.016 and 0.024 s^{-1}, for the adsorption layer formed from a 0.1 wt % Supersap solution (+ 10 mM NaCl + 0.01 wt % NaN_3) in a Langmuir trough.

Let us emphasize that some of these results are far from trivial and deserve further investigation. A high surface elasticity is typically observed with poorly soluble surfactants, such as long-chain fatty acids and lipids, which aggregate or precipitate in the bulk at very low concentrations. In contrast, saponins are rather water-soluble (above 10 wt %) and have a high cmc, which makes them unique within the realm of available surfactants and explains why the saponins are suitable for such a wide range of applications. It has already been shown that the high surface elasticity of saponins affects the foam film thinning,[35] significantly reduces the rate of Ostwald ripening,[61] and modifies the viscous friction in flowing foams (unpublished results), as compared to conventional surfactants. This peculiar behavior of saponins also makes them a very interesting model system for studying foam and emulsion dynamics.

The very high dilatational elasticity of the adsorption saponin layers cannot be explained by the formation of a solid condensed phase in the adsorption layer (as in the case of fatty acids)[62] because the shear elasticity of the layer is rather low and it easily flows upon shear deformation (manuscript in preparation). The detailed molecular mechanisms leading to these highly elastic adsorption layers are not clear at the moment. The most probable molecular interpretation of the elastic behavior of these layers is the stretching of the H bonds formed between the glycoside chains of the neighboring adsorbed molecules with related conformational changes in the saponin molecules. Computer modeling of the interactions between the neighboring molecules in the adsorption layer would be very useful in analyzing this mechanism of surface elasticity and its dependence on the molecular structure of the adsorbed species, which could be relevant to other natural surfactants as well.

Last but not least, the failure of the DSA method to provide correct results about the surface rheological properties of the saponin layers should be a warning message for anyone interested in the dynamic properties of rigid surface layers, such as those composed of solid particles, lipids, fatty acids, monoglycerides, catanionic surfactants, and some proteins. The reasons for the observed problems of the DSA method should be analyzed in more detail to define the limits of application for such systems.

■ ASSOCIATED CONTENT

Supporting Information. Experimental results from the expanding drop method with a 0.1 wt % Supersap solution: surface stress as a function of surface deformation. This material is available free of charge via the Internet at http://pubs.acs.org.

■ AUTHOR INFORMATION

Corresponding Author

*Phone: (+359-2) 962 5310. Fax: (+359-2) 962 5643. E-mail: nd@lcpe.uni-sofia.bg.

■ ACKNOWLEDGMENT

We are grateful to Dr. J. Sainz (formerly at Desert King, Chile; currently at Prodalysa Ltda., Chile) for providing the saponin samples and for numerous useful discussions, to Mrs. B. Nenova for the experiments with the Langmuir trough, and to Dr. Y. Atanasov and Mrs. N. Politova for constructing the computer models of the saponin molecules (all from Sofia University, Bulgaria). This study was supported by Unilever R&D Vlaardingen, The Netherlands.

■ REFERENCES

(1) Hostettmann, K.; Marston, A. *Saponins*; Cambridge University Press: New York, 1995.

(2) Guglu-Ustundag, O.; Mazza, G. Saponins: properties, applications and processing. *Crit. Rev. Food Sci. Nutr.* **2007**, *47*, 231.

(3) Micich, T. J.; Foglia, T. A.; Holsinger, V. H. Polymer-supported saponins: an approach to cholesterol removal from butteroil. *J. Agric. Food Chem.* **1992**, *40*, 1321.

(4) Ash, M.; Ash, I. *Handbook of Food Additives*; Synapse Information Resources Inc.: New York, 2002.

(5) Cheeke, P. R. Actual and potential applications of *Yucca schidigera* and *Quillaja saponaria* saponins in human and animal nutrition. *Proc. Am. Soc. Anim. Sci.* **1999**, *E9*, 1−10.

(6) Oakenfull, D. Saponins in food - a review. *Food Chem.* **1981**, *6*, 19.

(7) Blunden, G.; Culling, M. C.; Jewers, K. Steroidal sapogenins: a review of actual and potential plant sources. *Trop. Sci.* **1975**, *17*, 139.

(8) Brown, R. The natural way in cosmetics and skin care. *Chem. Mark. Rep.* **1998**, *254*, FR8.

(9) Bomford, R.; Stapleton, M.; Winsor, S.; Beesly, J. E.; Jessup, E. A.; Price, K. R.; Fenwick, G. R. Adjuvancity and ISCOM formation by structurally diverse saponins. *Vaccine* **1992**, *10*, 572.

(10) Oakenfull, D. Soy protein, saponins and plasma cholesterol. *J. Nutr.* **2001**, *131*, 2971.

(11) Kim, S.-W.; Park, S.-K.; Kang, S.-I.; Kang, H.-C.; Oh, H.-J.; Bae, C.-Y.; Bae, D.-H. Hypocholesterolemic property of *Yucca schidigera* and *Quillaja saponaria* extracts in human body. *Arch. Pharm. Res.* **2003**, *26*, 1042.

(12) Ros, E. Intestinal absorption of triglycerides and cholesterol. Dietary and pharmacological inhibition to reduce cardiovascular risk. *Artherosclerosis* **2000**, *151*, 357.

(13) Kensil, C. R.; Mo, A. X.; Truneh, A. Current vaccine adjuvants: an overview of a diverse class. *Front. Biosci.* **2004**, *9*, 2972.

(14) Rao, A. V.; Sung, M.-K. Saponins as anticarcinogens. *J. Nutr.* **1995**, *125*, 717.

(15) Panagin Pharmaceuticals Inc website: www.panagin.com/publications.html.

(16) Jenkins, K. J.; Atwal, A. S. Effects of dietary saponins on fecal bile acids and neutral sterols, and availability of vitamins A and E in the chick. *J. Nutr. Biochem.* **1994**, *5*, 134.

(17) Southon, S.; Wright, A. J. A.; Price, K. R.; Fairweather-Tait, S. J.; Fenwick, G. R. The effect of three types of saponin on iron and zinc absorption from a single meal in the rat. *Br. J. Nutr.* **1988**, *59*, 389.

(18) Indena S. p. A. website. Horse chestnut saponins. www.indena.com/pdf/horse_chestnut_saponins.pdf.

(19) Olmstead, M. J. Organic toothpaste containing saponin. U.S. Patent 6,485,711 B1, 2002.

(20) Bombardelli, E.; Morazzoni, P.; Cristoni, A.; Seghizzi, R. Pharmaceutical and cosmetic formulations with antimicrobial activity. U.S. Patent Application 2001/0046525 A1, 2001.

(21) Das, D.; Panigrahi, S.; Misra, P. K.; Nayak, A. Effect of organized assemblies. Part 4. Formulation of highly concentrated coal-water slurry using a natural surfactant. *Energy Fuels* **1965**, *1008*, 22.

(22) Oakenfull, D. Aggregation of saponins and bile acids in aqueous solution. *Aust. J. Chem.* **1986**, *39*, 1671.

(23) Mitra, S.; Dungan, S. R. Micellar properties of quillaja saponin. 1. Effects of temperature, salt and pH on solution properties. *J. Agric. Food Chem.* **1997**, *45*, 1587.

(24) Mitra, S.; Dungan, S. R. Micellar properties of quillaja saponin. 2. Effect of solubilized cholesterol on solution properties. *Colloids Surf., B* **2000**, *17*, 117.

(25) Mitra, S.; Dungan, S. R. Cholesterol solubilization in aqueous micellar solutions of quillaja saponin, bile salts, or nonionic surfactants. *J. Agric. Food Chem.* **2001**, *49*, 384.

(26) Wang, Z.-W.; Gu, M.-Y.; Li, G.-Z. Surface properties of gleditsia saponin and synergisms of its binary system. *J. Disper. Sci. Technol.* **2005**, *26*, 341.

(27) Tcholakova, S.; Denkov, N. D.; Ivanov, I. B.; Campbell, B. Coalescence stability of emulsions containing globular milk proteins. *Adv. Colloid Interface Sci.* **2006**, *123*−*126*, 259.
(28) Murray, B. S. Interfacial rheology of mixed food protein and surfactant adsorption layers with respect to emulsion and foam stability. In *Proteins at Liquid Interfaces*; Mobius, D., Miller, R., Eds.; Elsevier: Amsterdam, 1998.
(29) Murray, B. Interfacial rheology of food emulsifiers and proteins. *Curr. Opin. Colloid Interface Sci.* **2002**, *7*, 426.
(30) Denkov, N.; Tcholakova, S.; Golemanov, K.; Ananthpadmanabhan, K. P.; Lips, A. Role of surfactant type and bubble surface mobility in foam rheology. *Soft Matter* **2009**, *7*, 3389.
(31) Ibanoglu, E.; Ibanoglu, S. Foaming behavior of liquorice (Glycyrrhiza glabra) extract. *Food Chem.* **2000**, *70*, 333.
(32) Skurtys, O.; Aguilera, J. M. Formation of o/w macroemulsions with a circular microfluidic device using saponin and potato starch. *Food Hydrocolloids* **2009**, *23*, 1810.
(33) Blijdenstein, T. B. J.; De Groot, P. W. N.; Stoyanov, S. D. On the link between foam coarsening and surface rheology: why hydrophobins are so different. *Soft Matter* **2010**, *6*, 1799.
(34) Wojciechowski, K.; Piotrowski, M.; Popielarz, W.; Sosnowski, T. R. Short- and mid-term adsorption behaviour of *Quillaja* bark saponin and its mixtures with lysozyme. *Food Hydrocolloids* **2011**, *25*, 687.
(35) Anton, N.; Bouriat, P. Different surface corrugations occurring during drainage of axisymmetric thin liquid films. *Langmuir* **2007**, *23*, 9213.
(36) Dukhin, S. S.; Kretzschmar, G.; Miller, R. *Dynamics of Adsorption at Liquid Interfaces*; Elsevier: Amsterdam, 1995.
(37) Adamson, A. W.; Gast, A. P. *Physical Chemistry of Surfaces*, 6th ed.; Wiley: New York, 1997.
(38) *Drops and Bubbles in Interfacial Research*; Möbius, D., Miller, R., Eds.; Elsevier: Amsterdam, 1998.
(39) Rotenberg, Y.; Boruvka, L.; Neumann, A. W. Determination of surface tension and contact angle from the shapes of axisymmetric fluid interfaces. *J. Colloid Interface Sci.* **1983**, *93*, 169.
(40) Hoorfar, M.; Neumann, A. W. Recent progress in axisymmetric drop shape analysis (ADSA). *Adv. Colloid Interface Sci.* **2006**, *121*, 25–49.
(41) Song, B.; Springer, J. Determination of interfacial tension from profile of a pendant drop using computer-aided image processing. 2. Experimental. *J. Colloid Interface Sci.* **1996**, *184*, 77.
(42) Passerone, A.; Liggieri, L.; Rando, M.; Ravera, F.; Ricci, E. A new experimental method for measurement of the interfacial tension between immiscible fluids at zero bond number. *J. Colloid Interface Sci.* **1991**, *146*, 152.
(43) Liggieri, L.; Ravera, F. In *Drops and Bubbles in Interfacial Research*; Möbius, D., Miller, R., Eds.; Elsevier:Amsterdam, 1998; p 239.
(44) Russev, S. C.; Alexandrov, N.; Marinova, K. G.; Danov, K. D.; Denkov, N. D.; Lyutov, L.; Vulchev, V.; Bilke-Krause, C. Instrument and methods for surface dilatational rheology measurements. *Rev. Sci. Instrum.* **2008**, *79*, 1864.
(45) Alexandrov, N.; Marinova, K. G.; Danov, K. D.; Ivanov, I. B. Surface dilatational rheology measurements for oil/water systems with viscous oils. *J. Colloid Interface Sci.* **2009**, *339*, 545.
(46) Petkov, J.; Gurkov, T.; Campbell, B.; Borwankar, R. Dilatational and shear elasticity of gel-like protein layers on air/water interface. *Langmuir* **2000**, *16*, 3703.
(47) Gurkov, T. D.; Petkov, J. T.; Campbell, B.; Borwankar, R. P. Dilatational and Shear Rheology of Protein Layers on Water/Air Interface. In *Food Colloids, Fundamentals of Formulation*; Dickinson, E., Miller, R., Eds.; Royal Society of Chemistry: Cambridge, U.K., 2001; pp 181−190.
(48) Mulligan, C. N. Recent advances in the environmental applications of biosurfactants. *Curr. Opin. Colloid Interface Sci.* **2009**, *14*, 372.
(49) Schick, M. J. *Nonionic Surfactants: Physical Chemistry*; Marcel Dekker: New York, 1986.
(50) Rosen, M. J. *Surfactants and Interfacial Phenomena*; Wiley: New York, 1989.
(51) Gurkov, T. D.; Dimitrova, D. T.; Marinova, K. G.; Bilke-Crause, C.; Gerber, C.; Ivanov, I. B. Ionic surfactants on fluid interfaces: determination of the adsorption; role of the salt and the type of the hydrophobic phase. *Colloids Surf., A* **2005**, *261*, 29.
(52) Kralchevsky, P. A.; Danov, K. D.; Denkov, N. D. Chemical Physics of Colloid Systems and Interfaces. In *Handbook of Surface and Colloid Chemistry*; Birdi, K. S., Ed.; CRC Press: New York: 2008; p 197.
(53) Danov, K. D.; Kralchevsky, P. A.; Ananthapadmanabhan, K. P.; Lips, A. Interpretation of surface-tension isotherms of n-alkanoic (fatty) acids by means of the van der Waals model. *J. Colloid Interface Sci.* **2006**, *300*, 809.
(54) Kolev, V. L.; Danov, K. D.; Kralchevsky, P. A.; Broze, G.; Mehreteab, A. Comparison of the van der Waals and Frumkin adsorption isotherms for sodium dodecyl sulfate at various salt concentrations. *Langmuir* **2002**, *18*, 9106.
(55) Danov, K. D.; Kralchevsky, P. A.; Denkov, N. D.; Ananthapadmanabhan, K. P.; Lips, A. Mass transport in micellar surfactant solutions: 2. Theoretical modeling of adsorption at a quiescent interface. *Adv. Colloid Interface Sci.* **2006**, *119*, 17.
(56) Xu, H.; Melle, S.; Golemanov, K.; Fuller, G. Shape and buckling transitions in solid-stabilized drops. *Langmuir* **2005**, *21*, 10016.
(57) Gavranovic, G. T.; Kurtz, R. E.; Golemanov, K.; Lange, A.; Fuller, G. G. Interfacial rheology and structure of straight-chain and branched hexadecanol mixtures. *Ind. Eng. Chem. Res.* **2006**, *45*, 6880.
(58) Basheva, E. S.; Kralchevsky, P. A.; Danov, K. D.; Stoyanov, S. D.; Blijdenstein, T. B. J.; Pelan, E. G.; Lips, A. Self-assembled bilayers from the protein HFBII hydrophobin: nature of the adhesion energy. *Langmuir* **2011**, *27*, 4481.
(59) Basheva, E. S.; Kralchevsky, P. A.; Danov, K. D.; Ananthapadmanabhan, K. P.; Lips, A. The colloid structural forces as a tool for particle characterization and control of dispersion stability. *Phys. Chem. Chem. Phys.* **2007**, *9*, 5183.
(60) Christov, N. C.; Danov, K. D.; Kralchevsky, P. A.; Ananthapadmanabhan, K. P.; Lips, A. The maximum bubble pressure method: universal surface age and transport mechanisms in surfactant solutions. *Langmuir* **2006**, *22*, 7528.
(61) Tcholakova, S.; Mitrinova, Z.; Golemanov, K.; Denkov, N. D.; Vethamuthu, M.; Ananthpadmanabhan, K. P. Control of bubble Ostwald ripening in foams by using surfactant mixtures. *Langmuir*, submitted for publication.
(62) Golemanov, K.; Denkov, N. D.; Tcholakova, S.; Vethamuthu, M.; Lips, A. Surfactant mixtures for control of bubble surface mobility in foam studies. *Langmuir* **2008**, *24*, 9956.